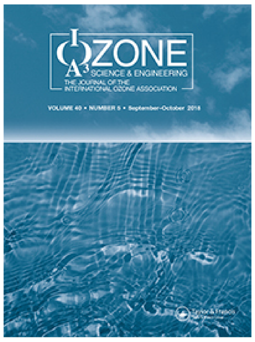

Taylor & Francis
Taylor & Francis Group

Ozone: Science & Engineering
The Journal of the International Ozone Association

ISSN: 0191-9512 (Print) 1547-6545 (Online) Journal homepage: http://www.tandfonline.com/loi/bose20

Reaction of ozone with polybenzimidazole (PBI)

Omran Omar, Bao Ha, Katerine Vega, Andrew Fleischer, Hyukin Moon, Joel Shertok, Alla Bailey, Michael Mehan, Surendra K. Gupta & Gerald A. Takacs

To cite this article: Omran Omar, Bao Ha, Katerine Vega, Andrew Fleischer, Hyukin Moon, Joel Shertok, Alla Bailey, Michael Mehan, Surendra K. Gupta & Gerald A. Takacs (2018) Reaction of ozone with polybenzimidazole (PBI), Ozone: Science & Engineering, 40:5, 392-398, DOI: 10.1080/01919512.2018.1446127

To link to this article: https://doi.org/10.1080/01919512.2018.1446127

OZONE: SCIENCE & ENGINEERING
2018, VOL. 40, NO. 5, 392–398
https://doi.org/10.1080/01919512.2018.1446127

Reaction of ozone with polybenzimidazole (PBI)

Omran Omar[a], Bao Ha[a], Katerine Vega[a], Andrew Fleischer[a], Hyukin Moon[a], Joel Shertok[a], Alla Bailey[a], Michael Mehan[b], Surendra K. Gupta[c], and Gerald A. Takacs[a]

[a]School of Chemistry and Materials Science, Rochester Institute of Technology, Rochester, NY, USA; [b]Xerox Analytical Services, Xerox Corporation, Webster, NY, USA; [c]Department of Mechanical Engineering, Rochester Institute of Technology, Rochester, NY, USA

ABSTRACT
Ozone reacted with the polybenzimidazole (PBI) film surface and X-ray photoelectron spectroscopy (XPS) detected a rapid increase in O atom concentration up to a saturation level of 27 ± 1 atomic %. Atomic force microscopy measurements showed little change in surface roughness. The water contact angle of the treated film decreased by ca. 60% compared to untreated PBI film indicating an increase in hydrophilicity and hydrogen bonding due the formation of the polar oxygenated functional groups. With treatment, the curve fitting of the XPS chemical states showed a decrease in the C–C sp^2, C–C sp^3, and C=N functional groups, and an increase in C–N, C=O, O–C=O, O–(C=O)–O, and N–C=O moieties which were explained using mechanisms associated with the dissociation of the primary ozonide formed from the addition of ozone to the C=C and C=N bonds and reaction with the amine groups in PBI. Washing the treated surface with water partially washed away the O concentration which indicated the formation of a weak boundary layer due to the breakage of bonds in the decomposition of the primary ozonide.

ARTICLE HISTORY
Received 20 November 2017
Accepted 18 February 2018

KEYWORDS
Advanced Oxidation; Ozone; Polybenzimidazole; Water Contact Angle; X-Ray Photoelectron Spectroscopy (XPS)

Poly[2,2′-*m*-(phenylene)-5,5′-bibenzimidazole], better known as polybenzimidazole (PBI), or meta-PBI, is a high-performance polymer consisting of benzimidazole units, as shown in Figure 1, having high thermal stability, chemical resistivity, and mechanical strength making it suitable for many applications (Li et al. 2009). PBI fibers are used in the fabrication of firefighters' suits (Davis et al. 2010; Wainright et al. 1995), aerospace space suits (Bhatnagar et al. 2011), as well as, in high temperature proton exchange membrane fuel cells (HT-PEMFCs) where PBI film is doped with phosphoric acid (H_3PO_4) (Kondratenko, Gallyamov, and Khokhlov 2012; Li et al. 2009; Quartarone and Mustarelli 2012; Wainright et al. 1995). The proton conductivity is a result of proton transfer via hydrogen bonding between phosphoric acid and the nitrogen-containing groups in PBI.

Fuel cells are electrochemical devices that convert chemical energy into electric energy (Bailey et al. 2015; Santhanam et al. 2016, 2017). In the case of HT-PEMFCs, they operate in a range of 180–200°C and are employed in stationary and automobile applications (Kordesch and Simader 1995; Li et al. 2009). When hydrogen is the fuel, the only by-products of HT-PEMFCs are water and heat which makes this type of fuel cell a promising environmentally friendly technology (Bailey et al. 2015; Santhanam et al. 2016, 2017). However, there are some drawbacks that need to be overcome to commercialize the HT-PEMFCs among them the loss of H_3PO_4 from the PBI membrane (Jakobsen et al. 2016; Kim, Yi, and Song 2012; Seel et al. 2009; Yu, Xiao, and Benicewicz 2008).

Interfacial properties are a key aspect for optimization of membrane electrode assemblies (Gubler and Scherer 2008) and to increase the uptake of the proton carrier the concentration of the polar group on the polymer backbone must be maximized (Chandan et al. 2013). Therefore, to increase the surface properties and retention of the phosphoric acid by hydrogen bonding, this research investigated the reaction of ozone with PBI film to produce polar functional groups.

The reaction on the top 2–5 nm of the polymer surface was characterized by X-ray photoelectron spectroscopy (XPS) which is often used to analyze for cleaning, ablation, cross-linking and chemical moieties when treated with ions, radiation, and plasma (Strobel, Lyons, and Mittal 1994). Water contact angle (CA) and atomic force microscopy (AFM) measurements were conducted to determine the increase in hydrophilicity and changes in surface roughness, respectively, with treatment time.

CONTACT Gerald A. Takacs ✉ gatsch@rit.edu School of Chemistry and Materials Science, Rochester Institute of Technology, Rochester, NY 14623, USA.
Color versions of one or more of the figures in the article can be found online at www.tandfonline.com/bose.

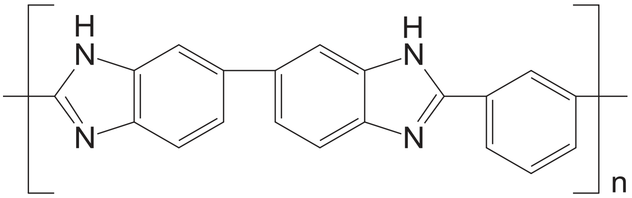

Figure 1. Poly[2,2′-*m*-(phenylene)-5,5′-bibenzimidazole] or *meta*-PBI.

Experimental

Materials

Commercially available 55μm thick PBI film (Celazole®) was purchased from PBI Performance Product, Inc. (Charlotte, NC) and cleaned with isopropanol in an ultrasonic bath for 20 min and stored in a desiccator, which contained calcium sulfate, for at least 24 h. The cleaned PBI film was then treated with ozone at a variety of treatment times.

Production of ozone

High purity oxygen (99.99%), at a flowrate of 43 standard cubic centimeters per minute (sccm), was fed into an Enaly Ozone Generator model 1000BT-12 (Shanghai, China), which has a high output corona discharge tube, to convert some of the oxygen into ozone. A 100% setting was used on the generator which corresponded to approximately 1.5% conversion of oxygen into ozone. The ozone was then flowed through a quartz cylindrical cell (2.54 cm diameter, 17.8 cm long) having high vacuum stainless steel fittings for placing the sample in and out of the cell. The exiting gas from the cell was passed through a solution of potassium iodide to convert the remaining ozone to oxygen prior to emission into the vacuum hood.

X-ray photoelectron spectroscopy

The samples were analyzed with a Physical Electronics Versaprobe II 5000 XPS that examined the top 2–5 nm of a sample's surface using a take-off angle of 45° between the sample and analyzer. A rectangular region of about 1400 μm by 600 μm was analyzed. The monochromatic Al K_α (1486 eV) X-ray beam irradiated the sample and the electron optics of the analyzer were focused to accept only photoelectrons emitted from the samples. The quantitative analyses are precise to within 5% relative for major constituents and 10% relative for minor constituents. The samples were charge neutralized with a dual beam charge neutralization system that utilizes both a cold cathode electron flood source (~1 eV) and a very low energy ion source (≤10 eV).

The high resolution C 1s and N 1s spectra were normalized to the peak intensities at the main hydrocarbon and C–N peaks, respectively, and curve fitting was performed using the C 1s and N 1s spectra for a cleaned and untreated PBI sample as the initial model. The process subtracted the control spectrum from that of the treated sample. The remainder spectrum was curve-fitted to determine the number of peaks, their binding energies, and peak widths resulting from treatment. The peaks from curve fitting the remainder spectrum were used to curve-fit the total treated spectrum. Any missing peaks, such as weak energy loss peaks, were then added to the curve fitting of the treated sample to achieve a good chi-square fit. A material balance was calculated to test if the results of the curve fitting agreed with the concentrations as determined from the quantitative analyses.

CA goniometry

Water CAs on the PBI films were measured using a Ramé-Hart model 250-F1 Standard Contact Angle Goniometer. The instrument includes fiber optic illuminator, 3-axis specimen stage with leveling, U1 Series SuperSpeed digital camera, and DROPimage Advanced software. During the CA measurement, the intensity of illuminator was set at 70%. The samples were placed on double-sided tape to keep the surface flat. A micropipette was used to deposit a 10-μL deionized water droplet on the surface. As soon as the water droplet was placed on the film, a picture was captured by the U1 Series Camera. The left-side and the right-side CAs were measured by the functioning DROPimage CA program. The standard deviation of the measurements was about ±2.5°.

Atomic force microscopy

Surface roughness was determined using a Bruker DI-3000 AFM in the tapping mode. For each specimen, a 15 μm × 15 μm image was obtained with the same Olympus OTESPA tip.

Results

XPS quantitative analyses and CA measurements

About 4 h were needed each time to pump six samples down to the pressure where XPS analysis could be completed. The elemental composition for the cleaned PBI film consisted of C, N, and O atoms. Although O is not in the PBI structure (Figure 1), measurements of 16 different untreated samples showed 6.6 ± 1.0 atomic % (at %) O. When treated with ozone (Figure 2), the oxygen concentration increased up to a saturation level of 27 ± 1 at %, the

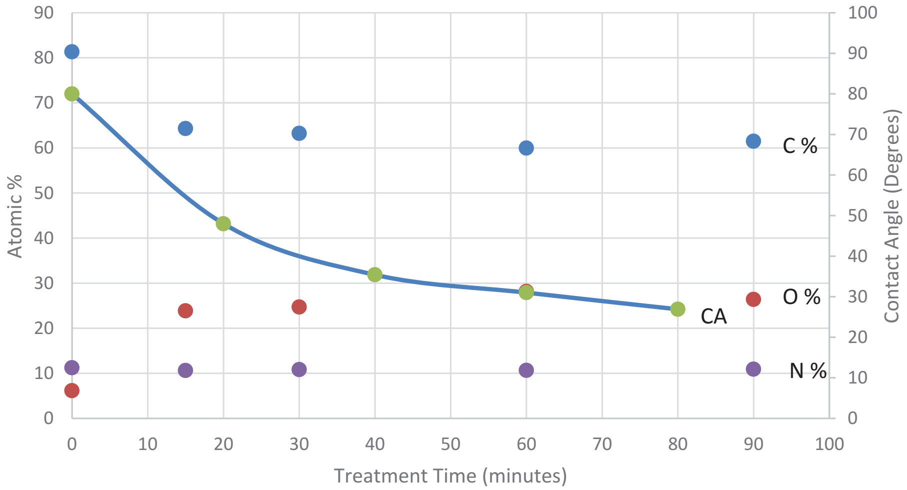

Figure 2. Quantitative XPS (at %) and contact angle (CA) results for PBI treated with ozone as a function of treatment time.

carbon concentration decreased by about the same amount, and the nitrogen composition on the surface decreased slightly by 0.8 at %. The increase in O atoms on the surface resulted in ca. 60% decrease in the water CA (Figure 2) making the surface more hydrophilic with treatment. Washing the treated samples with distilled water decreased the saturation level to 13 at % O.

XPS chemical state analysis

Figures 3 and 4 show the overlapped C 1s and N 1s spectra for the control and treated samples reported in Figure 2.

The O 1s spectra were broad Gaussian peaks which did not provide any additional information than the C 1s and N 1s spectra.

Curve fitting of the C 1s and N 1s spectra were accomplished using the binding energies for the chemical species given in Tables 1 and 2. With increasing treatment time, there are significant decreases in the concentrations of C–C sp^2, C–C sp^3, and C=N groups, and increases in the concentration of C=O, O–C=O, O–(C=O)–O, C–N, and N–C=O containing moieties accounting for the C 1s and N 1s peaks changing from a single peak to dual peaks as shown in Figures 3 and 4.

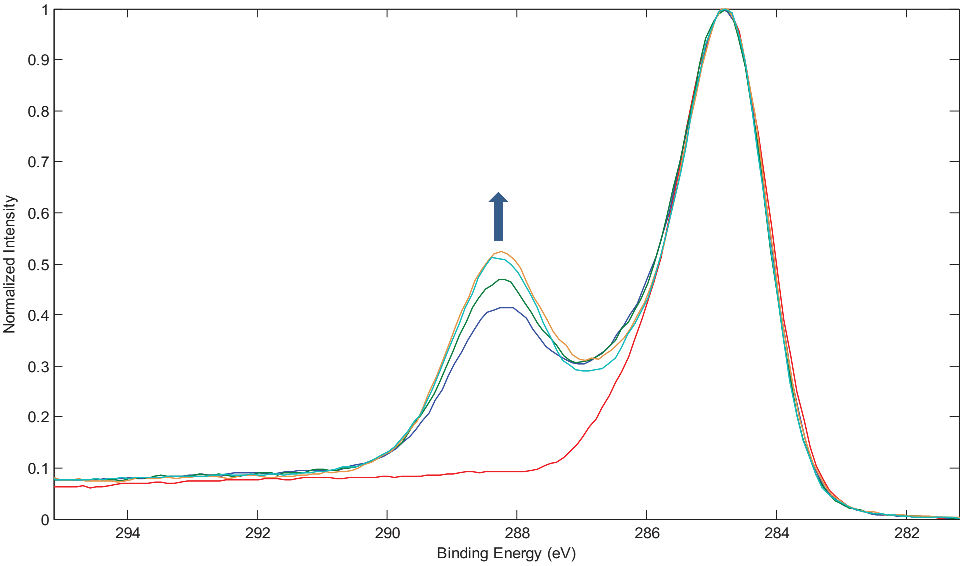

Figure 3. Overlapped C 1s spectra for control and ozone-treated PBI samples. The arrow indicates increasing treatment time for 0, 15, 30, 60, and 90 min.

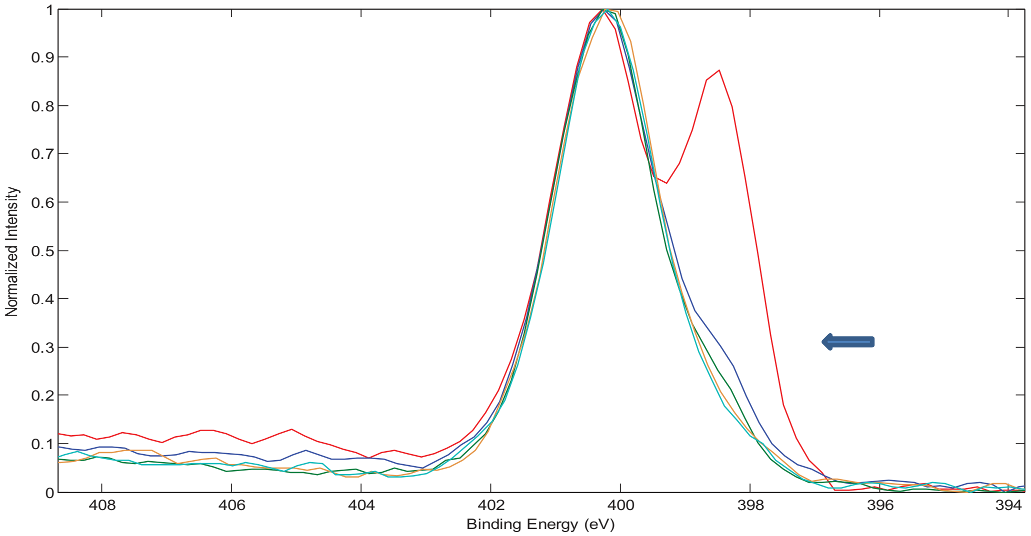

Figure 4. Overlapped N 1s spectra for control and ozone-treated PBI samples. The arrow indicates increasing treatment time for 0, 15, 30, 60, and 90 min.

Table 1. Assignments (Beamson and Briggs 1991) and areas for C 1s peaks as determined by curve fitting the spectra for PBI treated with ozone as a function of treatment time.

Binding energy (eV)	Species	0 min	10 min	30 min	90 min
284.6	C–C sp^2	56.2	34.3	35.8	32.2
285.1	C–C sp^3	17.4	16.5	10.4	10.4
285.7	C–N=	8.0	2.8	5.7	5.6
286.0	C–O–C, 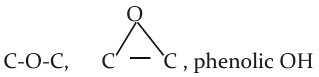 , phenolic OH	10.4	10.4	9.0	8.7
287.0	C=O, aldehyde	2.8	6.4	7.0	7.7
287.9	N–C=O	1.0	9.7	9.9	12.6
288.6	O–C=O, carboxylic acid	1.9	16.3	18.0	17.7
289.8	O = C–O–C = O, O–(C=O)–O	1.2	3.0	3.7	4.5
292.0	Energy loss	1.2	0.6	0.4	0.7

Table 2. Assignments (Beamson and Briggs 1991; Losito et al. 2005) and areas for N 1s peaks as determined by curve fitting the spectra for PBI treated with ozone as a function of treatment time.

Binding energy (eV)	Species	0 min	10 min	30 min	90 min
398.4	C=N	40.4	14.6	13.7	14.2
400.2	C–N	53.1	79.7	81.1	79.2
402.0	N–O	6.5	5.6	5.2	6.5

Surface topography for PBI treated with ozone

The root mean squared roughness factors reported in nanometers for the AFM images shown in Figure 5 are within one standard deviation of each other indicating no significant changes in surface topography with treatment time.

Discussion

Because the AFM measurements detected little change in surface roughness of the PBI samples treated with ozone (Figure 5), the observed increase in hydrophilicity (Figure 2) was due mainly to the chemical changes on the surface (Tables 1 and 2).

There have been few previous studies of the reaction of ozone with PBI. Ozone is well known to oxidize across unsaturated C–C sp^2 bonds to form a primary ozonide (Finlayson-Pitts and Pitts 2000), as has been reported for the ozonation of benzene (Wen et al. 2009), polystyrene (Al Abdulal et al. 2015), and carbon nanotubes (Banerjee and Wong 2002; Lu et al. 2002). Initially, ozone adds across the sp^2-hybridization which then undergoes O–O and C–C bond cleavage to form the carbonyl-containing groups observed in this study and a Criegee intermediate (Figure 6) (Finlayson-Pitts and Pitts 2000). One mechanism for the decomposition of the Criegee intermediate is the formation of ester groups (O–C=O) and the release of CO_2 (Finlayson-Pitts and Pitts 2000). Another pathway of the peroxy Creigee intermediate is a hydroperoxy channel (Finlayson-Pitts and Pitts 2000) which has been used to achieve polymer/carbon nanotube composites (Chang and Liu 2010), PBI-functionalized multi-walled

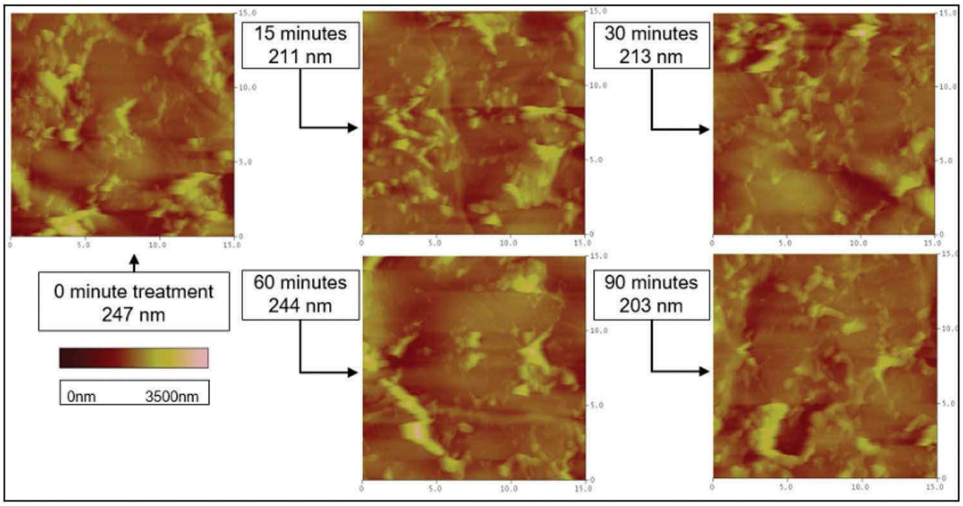

Figure 5. AFM surface topographic images after ozone treatment of PBI film for 0, 15, 30, 60 and 90 min showing the root mean squared roughness factors in nanometers.

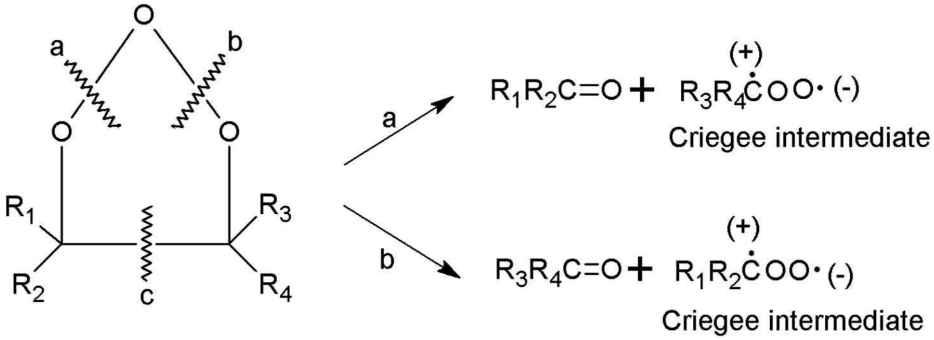

Figure 6. Decomposition of primary ozonide (Finlayson-Pitts and Pitts 2000).

carbon nanotubes (Suryani et al. 2011), and silica nanoparticles (Suryani et al. 2012).

The chemical structure for pure PBI (Figure 1) predicts the N 1s spectrum should deconvolute into equal areas for the imine, C=N, and amine, N–H, functional groups. However, since there is oxygen in the untreated samples (6.6 ± 1.0 at % O), oxygen appears in the functional groups for the control (Tables 1 and 2), such as, in the presence of an N–O peak appearing at 402.0 eV (Losito et al. 2005). Also, water is strongly adsorbed to the imine group in PBI (Samms, Wasmua, and Savinelli 1996) which may contribute to the lowering of the imine peak area and the presence of the N–O moiety. The adsorption of water may account for the difficulty in pumping down the PBI samples for XPS analysis.

Figure 7 displays the addition of ozone to the imine group in PBI and possible decomposition steps. Cleavage of the two peroxy O–O bonds (marked as "a" and "b" in Figure 7) and the N–C bond (marked as "c" in Figure 7) form different reaction products. Breakage of the "a" bond would result in a nitro, N=O, functional group having a binding energy of 406.9 eV (Monjushiro, Murata, and Ikeda 1985),which is not detected in this research (Figure 4, Table 2) while scission of the "b" bond produces the N–C=O group that is observed by the curve fitting results in Table 1. Similar to the loss of CO_2 by the Criegee intermediate, the other product of the "b" bond breakage may release gaseous NO_2 since there is no detection of the N=O functional group by XPS.

There are few studies of the reaction of ozone with amine groups. Part of the mechanism for the reaction of ozone with dimethylamine is shown in Equation [1] to form $(CH_3)_2NOH^*$ which produces $CH_3N{=}CH_2$ either by losing water, Equation [2], or by decomposing to $(CH_3)_2N$, Equation [3], and then reacting with oxygen, Equation [4] (Finlayson-Pitts and Pitts 2000; Tuazon et al. 1994).

$$(CH_3)_2NH + O_3 - > (CH_3)_2NOH^* + O_2 \qquad (1)$$

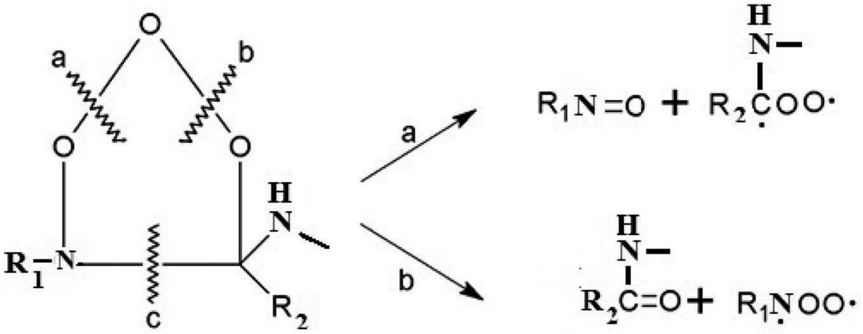

Figure 7. Ozonation of the imine moiety in PBI followed by decomposition of primary ozonide.

$$(CH_3)_2NOH^* - > CH_3N = CH_2 + H_2O \quad (2)$$

$$(CH_3)_2NOH^* - > (CH_3)_2N + OH \quad (3)$$

$$(CH_3)_2N + O_2 - > CH_3N = CH_2 + HO_2 \quad (4)$$

The OH and HO_2 free radicals, as formed in reactions [3] and [4], have been reported to oxidize the N–H bond in the imidazole ring of PBI forming quinine and dicarboxylic acid structures (Chang et al. 2009). In this study, the carboxylic acid/ester moieties increase with treatment time as well as the carbonate/anhydride functional groups (Table 1) which are often the highest oxidized form of bound carbon before CO_2 is released.

Washing the ozonized PBI samples with distilled water decreased the saturation level from 27 at % to 13 at % O probably because of breakage of the PBI backbone (step "c" in Figures 6 and 7) which would produce a weak boundary layer (WBL) similar to the ozonation of polystyrene (Lubarsky, Davidson, and Bradley 2004; Mahfoudh et al. 2010a, 2010b).

Conclusions

Ozone reacted with the PBI film surface and XPS detected a rapid increase in O atom concentration up to a saturation level of 27 ± 1 at %, a decrease in the C–C sp^2, C–C sp^3, and C=N functional groups, and an increase in C–N, C=O, O–C=O, O–(C=O)–O, and N–C=O moieties. AFM measurements showed little change in surface roughness. The water CA of the treated film decreased by ca. 60% compared to untreated PBI film indicating an increase in hydrophilicity and hydrogen bonding due the formation of the polar oxygenated functional groups. The mechanisms associated with the dissociation of the primary ozonide formed from the addition of ozone to the C=C and C=N bonds and reaction with the amines groups in PBI are described. Washing the treated surface with water lowered the O concentration because of the formation of a WBL due to breakage of bonds in the decomposition of the primary ozonide.

Acknowledgments

The authors gratefully acknowledge the help of Tom Allston with instrumentation and preparation of figures, and Nathan Eddingsaas for use of the ozone generator. This paper was presented at the 44th Annual Rochester Academy of Sciences Fall Scientific Paper Session, St. John Fisher College, Rochester, New York, November 11, 2017.

Disclosure

The authors declare no competing financial interest.

ORCID

Michael Mehan http://orcid.org/0000-0002-1217-8207
Surendra K. Gupta http://orcid.org/0000-0001-9941-645X

References

Al Abdulal, E., A. Khot, A. Bailey, M. Mehan, T. Debies, and G.A. Takacs. 2015. "Surface Characterizationof Polystyrene Treated with Ozone and Grafted with Poly(Acrylic Acid)." *Journal Adhesion Sciences Technological* 29 (1):1–11.

Bailey, A., L. Andrews, A. Khot, L. Rubin, J. Young, T.D. Allston, and G.A. Takacs. 2015. "Hydrogen Storage Experiments for an Undergraduate Laboratory Course-Clean Energy: Hydrogen/Fuel Cells." *Journal of Chemical Education* 92 (4):688–92.

Banerjee, S., and S.S. Wong. 2002. "Rational Sidewall Functionalization and Purification of Single-Walled Carbon Nanotubes by Solution-Phase Ozonolysis." *Journal Physical Chemical* B106:12144–51.

Beamson, G., and D. Briggs. 1991. *High Resolution XPS of Organic Polymers*. Chichester, West Sussex: Wiley.

Bhatnagar, N., D. Pyngrope, J. Rajiv, B. Sangeeta, P.H. Shantanu, V.T. Bui, and H. Bonin. 2011. "Electron Beam Modification of Space Durable Polymeric Nano-Adhesive Bonding of Ultra-High Temperature Resistant Polymer." *Journal Polymer Engineering* 31 (4):381–86.

Chandan, A., M. Hattenberger, A. El-Kharouf, S. Du, A. Dhir, V. Self, B.G. Pollet, A. Ingram, and W. Bujalski. 2013. "High Temperature (HT) Polymer Electrolyte Membrane Fuel Cells (PEMFC) – A Review." *Journal of Power Sources* 231:264–78.

Chang, C-M., and Y-L. Liu. 2010. "Functionalization of Multi-Walled Carbon Nanotubes with Non-Reactive Polymers through an Ozone-Mediated Process for the Preparation of a Wide Range of High Perform-Ance Polymer/Carbon Nanotube Composites." *Carbon* 48:1289–97.

Chang, Z., H. Pu, D. Wan, L. Liu, J. Yuan, and Z. Yang. 2009. "Chemical Oxidative Degradation of Polybenzmidazole in Simulated Environment of Fuel Cells." *Polymer Degradation Stability* 94:1206–12.

Davis, R., J. Chin, C-C. Lin, and S. Petit. 2010. "Accelerated Weathering of Polyaramid and Polybenzimid-Azole Firefighter Protective Clothing Fabrics." *Polymer Degradation Stability* 95 (9):1642–54.

Finlayson-Pitts, B.J., and J.N. Pitts. 2000. *Chemistry of the Upper and Lower Atmosphere*. New York, NY: Academic Press.

Gubler, L., and G.G. Scherer. 2008. "A Proton-Conducting Polymer Membrane as Solid Electrolyte – Function and Required Properties." *Advancement Polymer Sciences* 215:1–14.

Jakobsen, M.T.D., J.O.J. Jensen, L.N. Cleemann, and Q. Li. 2016. "Durability Issues and Status of PBI-Based Fuel Cells." In *High Temperature Polymer Electrolyte Membrane Fuel Cells*, edited by Q. Li, D. Aili, H.A. Hjuler, and J.O. Jensen, 487–501. Switzerland: Springer International.

Kim, J-R., J.S. Yi, and T-W. Song. 2012. "Investigation of Degradation Mechanisms of a High-Temperature Polymer-Electrolyte-Membrane Fuel Cell Stack by Electrochemical Impedance Spectroscopy." *Journal of Power Sources* 220:54–64.

Kondratenko, M. S., M.O. Gallyamov, and A.R. Khokhlov. 2012. "Performance of High Temperature Fuel Cells with Different Types of PBI Membranes as Analysed by Impedance Spectroscopy." *International Journal Hydrogen Energy* 37 (3):2596–602.

Kordesch, K.V., and G.R. Simader. 1995. "Environmental Impact of Fuel Cell Technology." *Chemical Reviews* 95 (1):191–207.

Li, Q., J.O. Jensen, R.F. Savinell, and N.J. Bjerrum. 2009. "High Temperature Proton Exchange Membranes Based on Polybenzimidazoles for Fuel Cells." *Progress Polymer Sciences* 34 (5):449–77.

Losito, L., C. Malitesta, I. de Bari, and C-D. Calvano. 2005. "X-Ray Photoelectron Spectroscopy Characterization of Poly(2,3-Diaminophenazine) Films Electrosynthesised on Platinum." *Thin Solid Films* 473:104–13.

Lu, X., L. Zhang, X. Xu, N. Wang, and Q. Zhang. 2002. "Can the Sidewalls of Single-Walled Nanotubes Be Ozonized?" *Journal Physical Chemical* B106:2136–39.

Lubarsky, G.V., M.R. Davidson, and R.H. Bradley. 2004. "Elastic Modulus, Oxidation Depth and Adhesion Force of Surface Modified Polystyrene Studied by AFM and XPS." *Surface Sciences* 558:135–44.

Mahfoudh, A., J. Barbeau, M. Moisan, A. Leduc, and J. Seguin. 2010a. "Biocidal Action of Ozone-Treated Polystyrene Surfaces on Vegetative and Sporulated Bacteria." *Applications Surface Sciences* 256:3063–72.

Mahfoudh, A., F. Poncin-Epaillard, M. Moisan, and J. Barbeau. 2010b. "Effect of Dry-Ozone Exposure on Different Polymer Surfaces and Their Resulting Biocidal Action on Sporulated Bacteria." *Surface Sciences* 604:1487–93.

Monjushiro, H., K. Murata, and S. Ikeda. 1985. "Reduction of Nitrobenzenes on Thin Aluminum Oxide Utilized in Inelastic Electron Tunneling Spectroscopy." *Bulletin Chemical Social Japan* 58 (3):957–61.

Quartarone, E., and P. Mustarelli. 2012. "Polymer Fuel Cells Based on Polybenzimidazole/H_3PO_4." *Energy & Environment Sciences* 5 (4):6436–44.

Samms, S.R., S. Wasmua, and R.F. Savinelli. 1996. "Thermal Stability of Proton Conducting Acid Doped Polybenzimiazole in Simulated Fuel Cell Environments." *Journal Electrochemistry Social* 143 (4):1225–32.

Santhanam, K.S.V., R.J. Press, M.J. Miri, A.V. Bailey, and G. A. Takacs. 2017. *Introduction to Hydrogen Technology*, 2nd ed. Hoboken, NJ: Wiley.

Santhanam, K.S.V., G.A. Takacs, M.J. Miri, A.V. Bailey, T.D. Allston, and R.J. Press. 2016. *Clean Energy: Hydrogen/Fuel Cells Laboratory Manual*. Hackensack, NJ: World Scientific.

Seel, D. C., B.C. Benicewicz, L. Xiao, and T.J. Schmidt. 2009. "High-Temperature Polybenzimidazole-Based Membranes." In *Handbook of Fuel Cells – Fundamentals, Technology and Applications*, edited by W. Vielstich, A. Lamm, and H.A. Gasteiger, 300–13. Chichester, UK: Wiley.

Strobel, S. M., C.S. Lyons, and K. L. Mittal. 1994. *Plasma Surface Modification of Polymers: Relevance to Adhesion*. Utrecht, The Netherlands: VSP.

Suryani, C-M. Chang, Y-L. Liu, and Y.M. Lee. 2011. "Polybenzimidazole Membranes Modified with Polyelectrolyte-Functionalized Multiwalled Carbon Nanotubes for Proton Exchange Membrane Fuel Cells." *Journal Materials Chemical* 21:7480–86.

Suryani, Y-N. Chang, J-Y. Lai, and Y-L. Liu. 2012. "Polybenzimidazole (PBI)-Functionalized Silica Nanoparticles Modified PBI Nanocomposite Membranes for Proton Exchange Membranes Fuel Cells." *Journal of Membrane Science* 403–404:1–7.

Tuazon, E.C., R. Atkinson, S.M. Aschmann, and J. Arey. 1994. "Kinetics of the Gas-Phase Reactions of O_3 with Amines and Related Compounds." *Researcher Chemical Intermediates* 20 (3–5):303–20.

Wainright, J. S., J-T. Wang, R.F. Savinelli, and M. Litt. 1995. "Acid-Doped Polybenzimidazoles: A New Polymer Electrolyte." *Journal Electrochemistry Social* 142 (7):L121–L123.

Wen, Z., Z. Wang, J. Zhou, and K. Cen. 2009. "A Theoretical Study on the Mechanism and Kinetics of the Reaction between Ozone and Benzene." *Ozone Sciences Engineering* 31:393–401.

Yu, S., L. Xiao, and B.C. Benicewicz. 2008. "Durability Studies of PBI-based High Temperature PEMFCs." *Fuel Cells* 8 (3–4):165–74.